The stress granule protein G3BP1 binds viral dsRNA and RIG-I to enhance interferon-β response

Received for publication, September 18, 2018, and in revised form, February 7, 2019 Published, Papers in Press, February 25, 2019, DOI 10.1074/jbc.RA118.005868

Susana Soo-Yeon Kim[‡1], **Lynette Sze**[‡], **and Kong-Peng Lam**[‡§¶2]

From the [‡]*Immunology Group, Bioprocessing Technology Institute, Agency for Science, Technology & Research (A*STAR), Singapore, the* [§]*Department of Microbiology & Immunology, Yong Loo Lin School of Medicine, National University of Singapore, Singapore, and* [¶]*School of Biological Sciences, Nanyang Technological University, Singapore*

Edited by Luke O'Neill

RIG-I senses viral RNA in the cytosol and initiates host innate immune response by triggering the production of type 1 interferon. A recent RNAi knockdown screen yielded close to hundred host genes whose products affected viral RNA-induced IFN-β production and highlighted the complexity of the antiviral response. The stress granule protein G3BP1, known to arrest mRNA translation, was identified as a regulator of RIG-I–induced IFN-β production. How G3BP1 functions in RIG-I signaling is not known, however. Here, we overexpress G3BP1 with RIG-I in HEK293T cells and found that G3BP1 significantly enhances RIG-I–induced *ifn-b* mRNA synthesis. More importantly, we demonstrate that G3BP1 binds RIG-I and that this interaction involves the C-terminal RGG domain of G3BP1. Confocal microscopy studies also show G3BP1 co-localization with RIG-I and with infecting vesicular stomatitis virus in Cos-7 cells. Interestingly, immunoprecipitation studies using biotin-labeled viral dsRNA or poly(I·C) and cell lysate–derived or *in vitro* translated G3BP1 indicated that G3BP1 could directly bind these substrates and again via its RGG domain. Computational modeling further revealed a juxtaposed interaction between G3BP1 RGG and RIG-I RNA-binding domains. Together, our data reveal G3BP1 as a critical component of RIG-I signaling and possibly acting as a co-sensor to promote RIG-I recognition of pathogenic RNA.

RIG-I (retinoic acid–inducible gene I) is an intracellular sensor of pathogen-associated molecular patterns (PAMPs)[3] and recognizes viral dsRNA in the cytosol (1). It triggers the production of type 1 interferon (IFN) to initiate the host innate anti-viral response (2, 3). It is known that RIG-I signaling involves the adaptor protein MAVS, which recruits the serine/threonine kinase TBK1 that subsequently phosphorylates and activates the transcription factor IRF3 (4). IRF3 dimerizes and translocates to the nucleus to induce *ifn-b* mRNA synthesis for IFN-β production (5). Although the overall scheme of RIG-I signaling has been elucidated, it remains possible that other molecules involved in RIG-I signal transduction have yet to be uncovered, and their precise roles in the pathway have yet to be determined. A recent integrative computational biology study indicates that a wide range of cellular processes and their associated regulators could affect viral RNA-induced IFN-β production (6), suggesting that the regulation of RIG-I signaling is likely to be highly complex. Close to a hundred genes were predicted to impact upon RIG-I signaling, and among them is G3BP1 (the gene encoding Ras-GTPase–activating SH3 domain–binding protein 1).

G3BP1 is a multidomain protein that is evolutionarily conserved from yeast to human (7). It contains, starting from the N terminus, a nuclear translocation factor-2–like domain, an acidic region, an RNA recognition motif (RRM), and a C-terminal glycine-rich RGG motif. The C-terminal half of G3BP1, comprising both RRM and RGG motifs, is involved in RNA recognition and exhibits DNA and RNA helicase activities (8). G3BP1 is a critical component of the mammalian cell stress granules (SGs). These are cytosolic nucleoprotein aggregate structures that are formed when cells are undergoing stress response and where host mRNAs are sequestered and translationally arrested (9, 10). Virus infection also represents a source of stress to mammalian cells. Infections by RNA viruses have been shown to induce or affect SG formation (11). A special class of SG, termed anti-viral SG, was formed during HIV infection and shown to attenuate viral replication (12). In addition, G3BP1 had been shown to be cleaved by viral-encoded proteases (13) during poliovirus and encephalomyocarditis virus infections (14). These studies suggested that G3BP1 could play an important role in host anti-viral response, but it is not clear biochemically, how G3BP1 functions during anti-viral signaling and in particular RIG-I signaling.

In this study, we provide biochemical evidence that G3BP1 is a critical component of the RIG-I signaling pathway. We show that G3BP1 could physically associate with RIG-I and viral dsRNA and that G3BP1 could synergize with RIG-I to induce the production of the important anti-viral cytokine, IFN-β. We also elucidated the RGG domain of G3BP1

This work was supported by the Agency for Science, Technology and Research. The authors declare that they have no conflicts of interest with the contents of this article.

This article contains Movie S1 and Figs. S1–S3.

[1] To whom correspondence may be addressed: Bioprocessing Technology Institute, 20 Biopolis Way, Singapore 138668, Singapore. E-mail: Susana_kim@bti.a-star.edu.sg.

[2] To whom correspondence may be addressed: Bioprocessing Technology Institute, 20 Biopolis Way, Singapore 138668, Singapore. E-mail: lam_kong_peng@bti.a-star.edu.sg.

[3] The abbreviations used are: PAMP, pathogen-associated molecular pattern; IFN, interferon; RRM, RNA recognition motif; SG, stress granule; tp(I·C), transfected poly(I·C); IP, immunoprecipitation or immunoprecipitated; RGG, arginine and glycine repeat; VSV, vesicular stomatitis virus; IB, immunoblot or immunoblotted; WCL, whole cell lysate; DAPI, 4′,6′-diamino-2-phenylindole; GAPDH, glyceraldehyde-3-phosphate dehydrogenase.

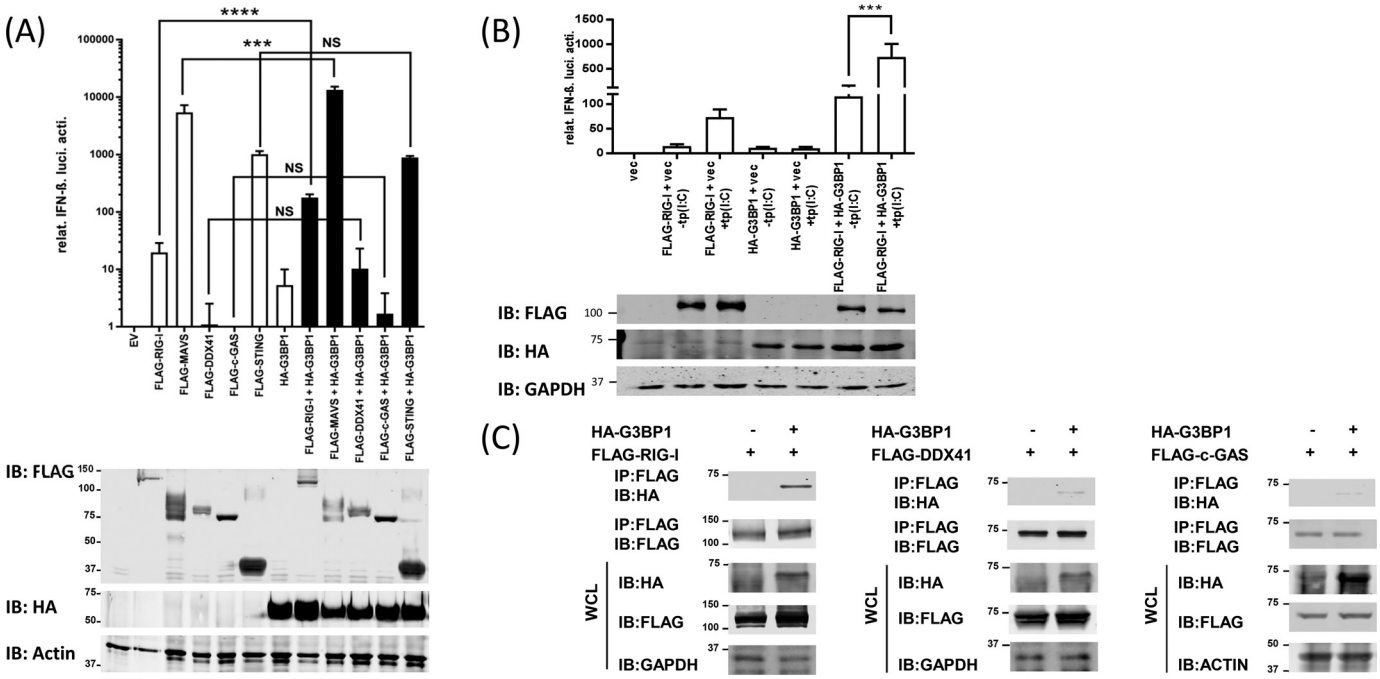

Figure 1. G3BP1 binds and enhances RIG-I–mediated *ifn-b* mRNA induction. *A*, G3BP1 enhances RIG-I–mediated induction of *ifn-b* mRNA synthesis. HEK293T cells were transiently transfected with vectors (*vec*) bearing HA-tagged G3BP1 or FLAG-tagged RIG-I, MAVS, DDX41, c-GAS, or STING; or various double combinations of HA-tagged G3BP1 with FLAG-tagged RIG-I, MAVS, DDX41, c-GAS, or STING; along with luciferase reporter bearing *ifn-b* promoter and *Renilla* control constructs. At 48 h post-transfection, the cells were analyzed for the induction of *ifn-b* promoter activity (*upper panel*). WCL was IB with anti-FLAG, anti-HA, or anti-actin antibodies to examine protein expression of the transfected gene constructs (*lower panel*). The data shown are means ± S.D. and are representative of triplicate independent experiments. Statistical significance was analyzed using unpaired two-tailed Student's *t* test, and *p* values of <0.05 were considered statistically significant. ****, $p < 0.0001$; *NS*, $p > 0.05$. *B*, poly(I·C) stimulation further enhances G3BP1 and RIG-I induction of *ifn-b* mRNA synthesis. HEK293T cells were transiently transfected with vectors bearing HA-tagged G3BP1 and/or FLAG-tagged RIG-I along with luciferase reporter bearing *ifn-b* promoter and *Renilla* control constructs. At 48 h post-transfections, the cells were left untreated or transfected with poly(I·C) (denoted +*tp(I·C)*) and analyzed 6 h later for *ifn-b* induction (*upper panel*). WCL was IB with anti-FLAG, anti-HA, or anti-actin antibodies to examine protein expression of the transfected gene constructs (*lower panel*). Statistical significance was analyzed as mentioned above. ****, $p < 0.0001$; ***, $p < 0.0005$; *NS*, $p > 0.05$. *C*, G3BP1 physically binds RIG-I. HEK293T cells were co-transfected with HA-tagged G3BP1 and FLAG-tagged RIG-I (*left panel*), FLAG-tagged DDX41 (*center panel*), or FLAG-tagged c-GAS (*right panel*) as indicated. WCL were IP and IB with relevant antibodies to examine protein–protein interactions. Anti-ACTIN and Anti-GAPDH blots were included as loading controls. *relat.*, relative; *luci.*, luciferase; *acti.*, activity.

to be important for its interaction with RIG-I and viral dsRNA.

Results

G3BP1 binds and enhances RIG-I induced ifn-b mRNA synthesis

A recent genomics-based discovery study utilizing an RNAi-screen revealed G3BP1 as a novel regulator of IFN-β production in response to viral RNA stimulation (6). The presence of cytosolic viral RNA activates RLR signaling (15). To examine whether G3BP1 participates in RIG-I signaling, we overexpressed G3BP1 alone or together with RIG-I in HEK293T cells and examined their induction of *ifn-b* mRNA synthesis using luciferase reporter assays. As seen in Fig. 1*A*, overexpression of G3BP1 or RIG-I alone induced some levels of IFN-β production. However, overexpression of G3BP1 and RIG-I together significantly activated *ifn-b* mRNA synthesis, suggesting that G3BP1 could act to enhance RIG-I induction of the anti-viral response. We also tested G3BP1 with MAVS, an adaptor downstream of RIG-I signaling, and likewise observed an increase in IFN-β production compared with MAVS-only transfected control, albeit to a lesser extent. However, we noted that G3BP1 was reported not to interact with MAVS (16), and any incremental *ifn-b* mRNA induction seen in our study could occur via RIG-1, because MAVS is an adaptor protein downstream of RIG-I (4). We next examined whether G3BP1 could participate in the signaling of other cytosolic sensors of PAMP and found that it did not have a significantly large effect, at least not to the same extent as that seen with RIG-I, when G3BP1 was overexpressed with either DDX41, c-GAS, or STING, all of which are involved in the sensing of pathogenic cytosolic DNA and also known to induce IFN-β production. Thus, G3BP1 appears to act in RIG-I signaling of IFN-β production.

To examine whether poly(I·C) stimulation could further enhance RIG-I/G3BP1-induced *ifn-b* promoter activity, we overexpressed G3BP1 alone or together with RIG-I in HEK293T cells and stimulated the cells with transfected poly(I·C) (denoted as tp(I·C)). As shown in Fig. 1*B*, tp(I·C) stimulation could further increase the induction of *ifn-b* mRNA synthesis. Because G3BP1 acted in concert with RIG-I to enhance IFN-β production, we hypothesized that G3BP1 could physically interact with RIG-I. To test this possibility, we overexpressed HA-tagged G3BP1 with FLAG-tagged RIG-I, c-GAS, or DDX41 in HEK293T cells and found that RIG-I strongly co-immunoprecipitated with G3BP1 (Fig. 1*C*). We also detected weak interactions between G3BP1 and DDX41 and G3BP1 and c-GAS. Because G3BP1 binds RIG-I the strongest, we decided to focus on elucidating the nature of G3BP1 and RIG-I interac-

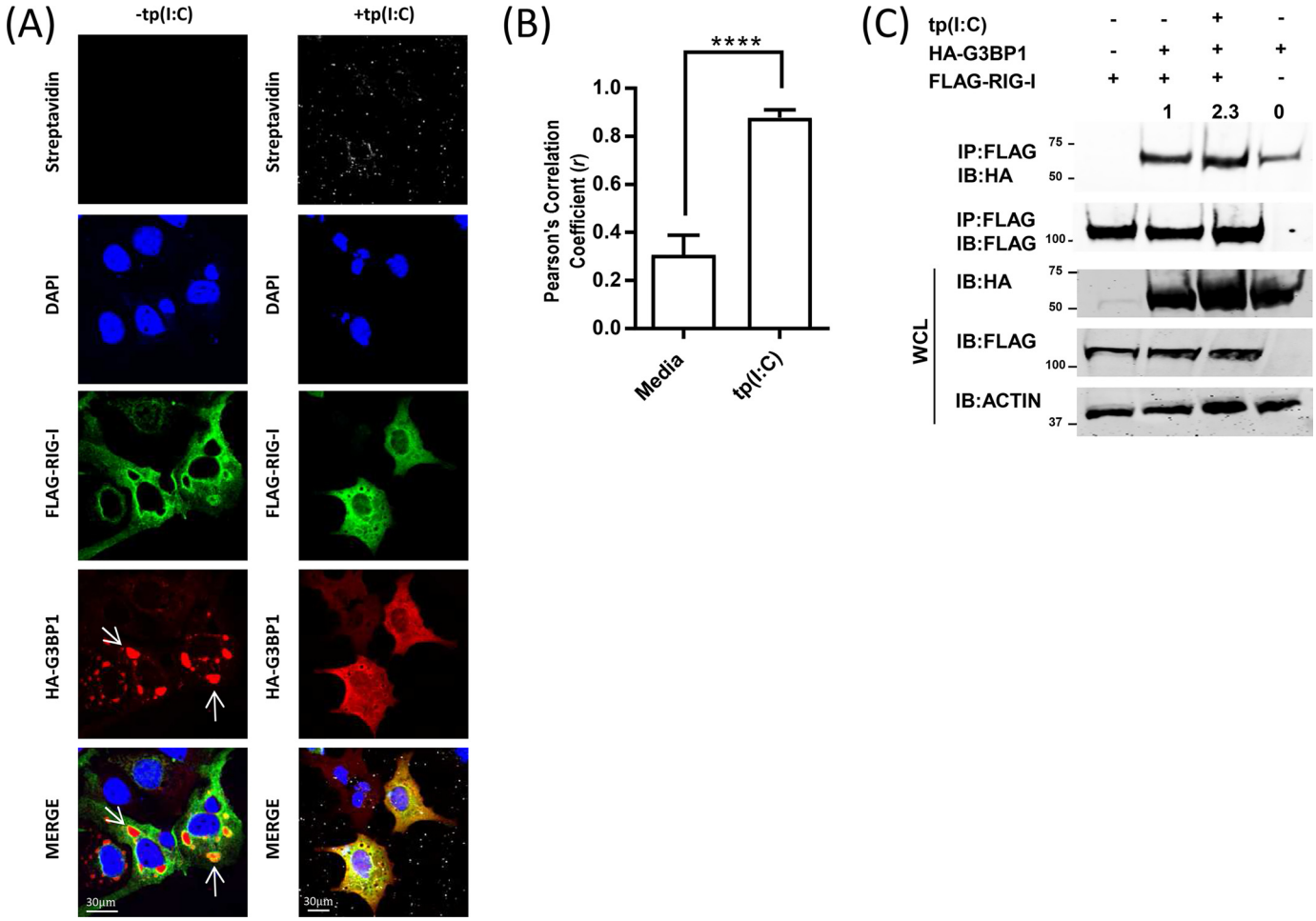

Figure 2. Examination of G3BP1 co-localization with RIG-I. *A*, confocal microscopy analysis of G3BP1 and RIG-I subcellular localization with and without poly(I·C) stimulation. Cos-7 cells were transiently transfected with HA-tagged G3BP1 and FLAG-tagged RIG-I, and at 24 h post-transfection, the cells were left untreated or transfected with biotin-conjugated tp(I·C) (denoted *+/−tp(I·C)*). HA-tagged G3BP1 (*red*) and FLAG-tagged RIG-I (*green*) were stained using fluorochrome-conjugated anti-HA or anti-FLAG antibodies. Biotin-conjugated poly(I·C) (*white*) was stained with fluorochrome-conjugated streptavidin. Nuclear staining was revealed with DAPI. *B*, quantification of RIG-I and G3BP1 co-localization using Pearson's correlation coefficient (*r*) ($n = 10$, Fig. S1). Statistical significance was analyzed as in Fig. 1. ****, $p < 0.0001$. *C*, increased G3BP1 and RIG-I binding upon tp(I·C) stimulation. Cos-7 cells were co-transfected with HA-tagged G3BP1 and FLAG-tagged RIG-I as indicated. At 24 h post-transfection, the cells were left untreated or transfected with tp(I·C). WCL were IP and IB with relevant antibodies to examine protein–protein interactions. Anti-actin antibodies were used as loading control for protein normalization in IB. Densitometry was performed on Western blotting images, and the numerical values obtained were subtracted from HA-G3BP1 (single transfection) sample and normalized to unstimulated sample, which was set as 1 (*lane 2*). The relative densitometry values are indicated *below* each corresponding lane.

tion in this study. Taken together, our data indicated that G3BP1 binds RIG-I to further promote IFN-β production.

Co-localization of G3BP1 and RIG-I

G3BP1 is known to induce the formation of SGs whereby host mRNAs are sequestered and stalled for translation during cell stress (17). On the other hand, RIG-I was shown to be recruited to cellular structures termed anti-viral stress granules upon viral infection (11). Because G3BP1 could bind RIG-I (Fig. 1*C*), we sought to determine whether the two proteins could co-localize in some cellular structures. We therefore overexpressed G3BP1 and RIG-I in Cos-7 cells (Fig. 2*A*) to determine the localization of these proteins in the absence or presence of tp(I·C). In the absence of tp(I·C) stimulation, overexpressed RIG-I was found mainly to be cytosolic, whereas G3BP1 was found in punctate or granule-like structures (*white arrows*). The two proteins co-localized to a certain extent (Fig. 2*A*, *left panel*, merge) and with the co-localization mainly confined to the perimeter of the granule structures. Interestingly, upon tp(I·C) stimulation, the localization of G3BP1 was altered such that the protein was no longer confined to the granular structures but rather became more diffusedly distributed throughout the cytosol (Fig. 2*A*, *right panel*). As a consequence, there also appeared to be increased co-localization of G3BP1 and RIG-I upon tp(I·C) stimulation (Fig. 2*B*). The spatial redistribution of G3BP1 upon tp(I·C) stimulation was evidenced with timed-lapse confocal microscopy showing the disassembly of the granules and the spread of G3BP1 in the cytosol (Fig. S2 and Movie S1). Co-immunoprecipitation (co-IP) experiment also supported increased G3BP-1/RIG-I co-localization and interaction upon tp(I·C) stimulation (Fig. 2*C*). Hence, our confocal microscopy and co-IP study together suggested that there was increased G3BP1 and RIG-I co-localization and interaction upon tp(I·C) stimulation, and this finding was consistent with the data in Fig. 1*B* showing increased *ifn-b* promoter activity in tp(I·C)-stimulated HEK293T cells overexpressing both G3BP1 and RIG-I.

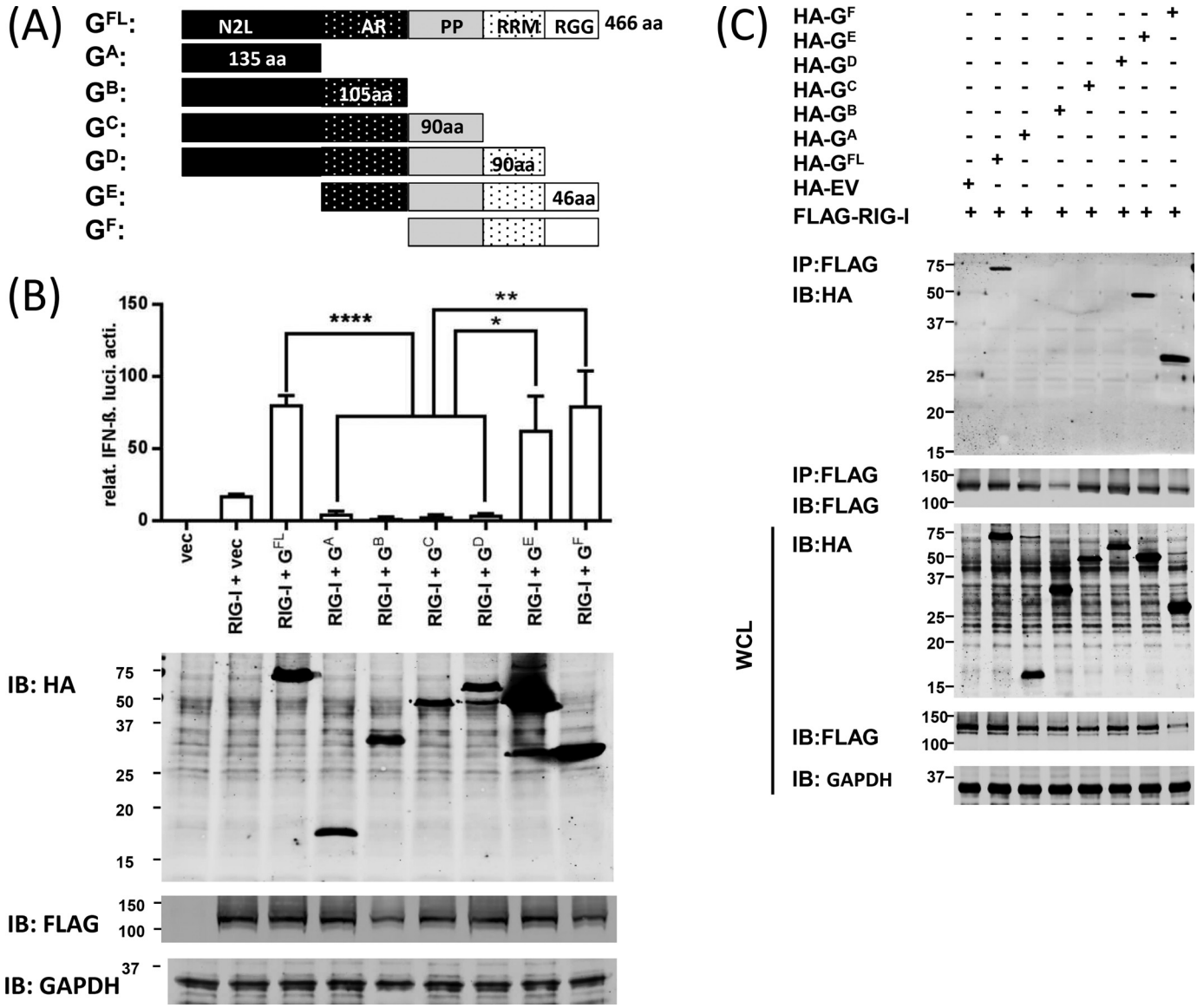

Figure 3. The C-terminal RGG domain of G3BP1 interacts with RIG-I. *A*, schematic representation of full-length (*FL*) and various mutant forms of G3BP1 depicting the various domains and amino acid (*aa*) sizes. *B*, the RGG domain of G3BP1 synergizes with RIG-I to induce *ifn-b* mRNA synthesis. HEK293T cells were transiently transfected with FLAG-tagged vector (*vec*) expressing RIG-I and HA-tagged vector expressing FL or various truncated forms of G3BP1 along with luciferase reporter bearing *ifn-b* promoter and *Renilla* control constructs. At 48 h post-transfection, the cells were analyzed for the induction of *ifn-b* promoter activity. Statistical significance was analyzed as in Fig. 1. *, $p < 0.05$; **, $p < 0.005$; ****, $p < 0.0001$. *C*, the RGG domain of G3BP1 binds RIG-I. Western blotting analyses of G3BP1 domain interactions with RIG-I. HEK293T cells were transfected with FLAG-tagged RIG-I and HA-tagged vectors expressing FL or various truncated forms of G3BP1. WCL were IP and IB with relevant antibodies as indicated to examine protein–protein interactions (*top panel*) or IB with relevant antibodies to examine protein expression of the transfected constructs (*bottom panel*). Anti-GAPDH blots were included as loading control. *relat.*, relative; *luci.*, luciferase; *acti.*, activity.

The C-terminal RGG domain of G3BP1 binds RIG-I

G3BP1 is a multidomain protein comprising an N-terminal nuclear transport factor 2-like (N2L), an acidic-rich (AR), a P*XX*P (PP), an RRM and, an arginine and glycine repeat (RGG) domains (8). Because G3BP1 could bind RIG-I, we next generated various truncated forms of G3BP1 (Fig. 3*A*) to determine which motif of G3BP1 mediates its binding of RIG-I. First, we overexpressed RIG-I with either full-length or various truncated forms of G3BP1 and examined their ability to induce *ifn-b* promoter activity using luciferase reporter assays in HEK293T cells. As shown in Fig. 3*B*, only truncated G^E and G^F mutants that harbored the RGG domain could induce *ifn-b* promoter activity to the same extent as full-length G3BP1 (G^{FL}) protein. The G^D mutant that shares other overlapping regions as the G^E and G^F mutants but lack the RGG domain could not activate *ifn-b* mRNA synthesis, further supporting the finding that the RGG domain is necessary. These data suggested that the RGG domain is critical for G3BP1 to act in concert with RIG-I to further induce *ifn-b* mRNA synthesis.

We next performed co-IP study to definitively establish whether the RGG domain of G3BP1 indeed mediates its binding to RIG-I. We overexpressed RIG-I alone or together with full-length or various mutants of G3BP1 in HEK293T cells and showed that only the full length and G^E and G^F variants of G3BP1 could co-IP with RIG-1 (Fig. 3*C*). Again G^D mutant that lacked the RGG domain could not physically bind RIG-I. Thus,

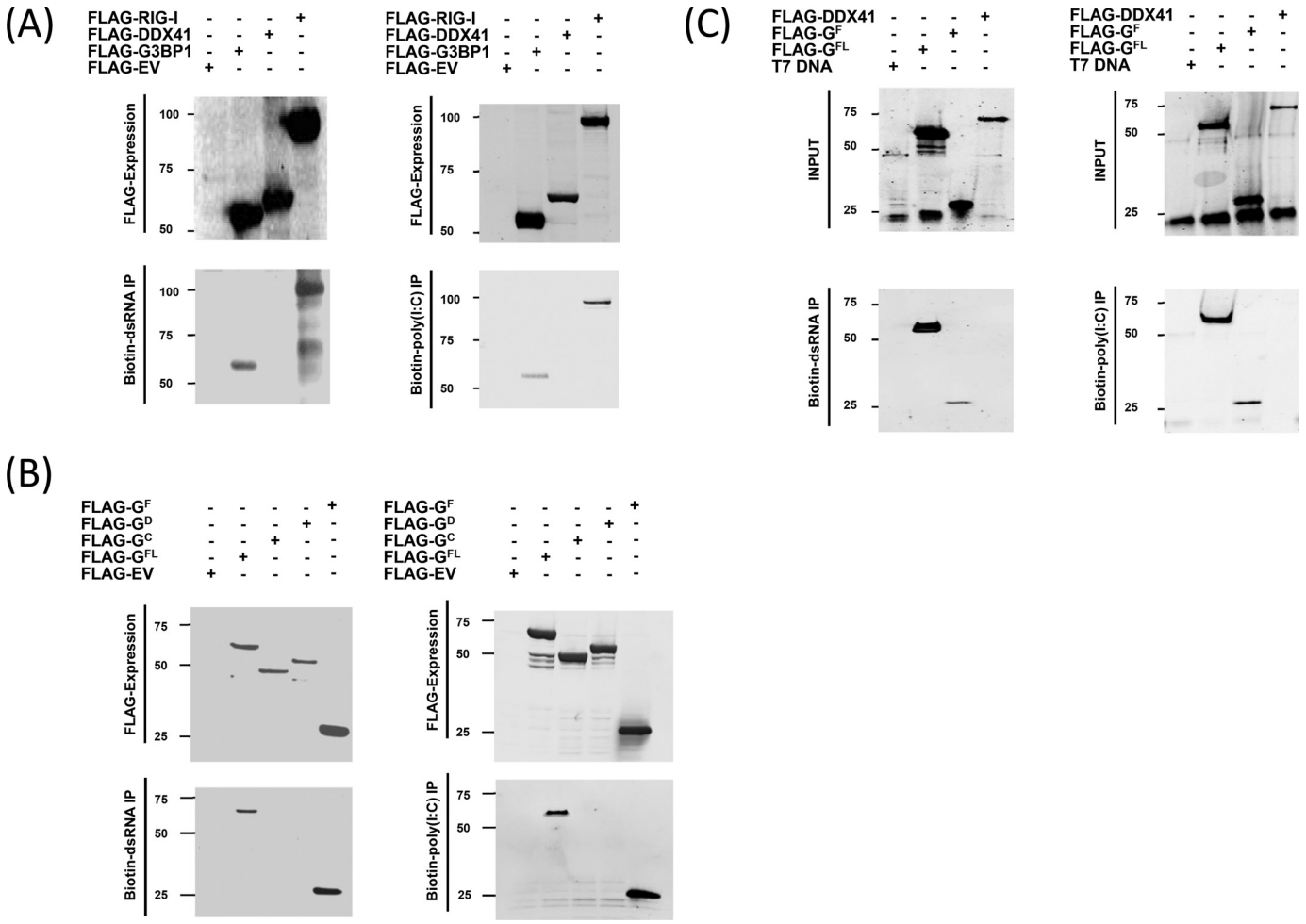

Figure 4. The C-terminal RGG domain of G3BP1 binds dsRNA and poly(I·C). Immunoblot analyses of G3BP1, RIG-I, and DDX41 (*A*) and various mutants of G3BP1 binding of dsRNA and poly(I·C) (*B*). WCL containing FLAG-tagged RIG-I, DDX41, and full-length or variants of G3BP1 were incubated with biotin-conjugated dsRNA or poly(I·C) and subsequently IP with streptavidin beads and probed with anti-FLAG antibody. WCL were also probed for expression of the FLAG-tagged proteins. *C*, immunoblot analyses of dsRNA and poly(I·C) binding by *in vitro* translated G3BP1^{FL}, G3BP1^{F}, and DDX41. The proteins were *in vitro* translated using a cell-free system and purified using FLAG IP. Biotin-conjugated dsRNA or poly(I·C) was incubated with purified G3BP1^{FL}, G3BP1^{F}, or DDX41 and subsequently, IP with streptavidin beads, and probed with anti-FLAG antibody. The *upper panel* indicated the expression of the *in vitro* translated FLAG-tagged proteins. Luciferase T7 control DNA is included as control.

the RGG domain of G3BP1 was demonstrated biochemically to be necessary to bind RIG-I, and this interaction is important for G3BP1 to further enhanced RIG-I induction of *ifn-b* promoter activity.

The C-terminal RGG domain of G3BP1 could bind poly(I·C) and viral dsRNA

G3BP1 was previously identified as an RNA-binding protein that regulates the turnover of host mRNA, as well as arresting and sequestering them in stress granules in times of cell stress (18, 19). Its RRM domain was found to be responsible for these functions (17). However, G3BP1 also possesses the RGG domain that was shown in other proteins such as FUS (20–22) and Caprin-1 (23) to be RNA-binding. We speculated that G3BP1 could bind viral RNA in addition to host mRNA, and either its RMM or RGG or both domains would be involved. To test this hypothesis, we employed biotin-conjugated poly(I·C) and HCV-dsRNA as substrates in a pulldown assay to examine the RNA-binding properties of G3BP1. RIG-I, which binds RNA and DDX41 that binds DNA, were used as positive and negative controls. As shown in Fig. 4*A*, G3BP1 and RIG-I but not DDX41 co-precipitated with HCV-dsRNA (*left panel*) and poly(I·C) (*right panel*) when lysates from cells overexpressing these proteins were incubated with the biotin-conjugated substrates. These data indicated that G3BP1 could bind viral dsRNA and poly(I·C).

We next proceeded to identify the motifs in G3BP1 that mediated the binding of HCV-dsRNA and poly(I·C). Toward this end, we incubated these two biotin-conjugated substrates with cell lysates expressing selected variant forms of G3BP1. As shown in Fig. 4*B*, the G^{F} variant that harbored the P*XX*P, RRM, and RGG domain could bind both poly(I·C) and HCV-dsRNA. However, the G^{D} variant that also harbored the PXXP and RRM but lacked the RGG domain could not bind. These data suggested that the RGG but not the RRM domain of G3BP1 mediated the binding of HCV-dsRNA and poly(I·C).

To definitively examine whether G3BP1 and its RGG domain could directly bind poly(I·C) and HSV dsRNA, we repeated the pulldown assays using *in vitro* translated G3BP1, G^{F} variant and DDX41 obtained via a cell-free system and found that indeed

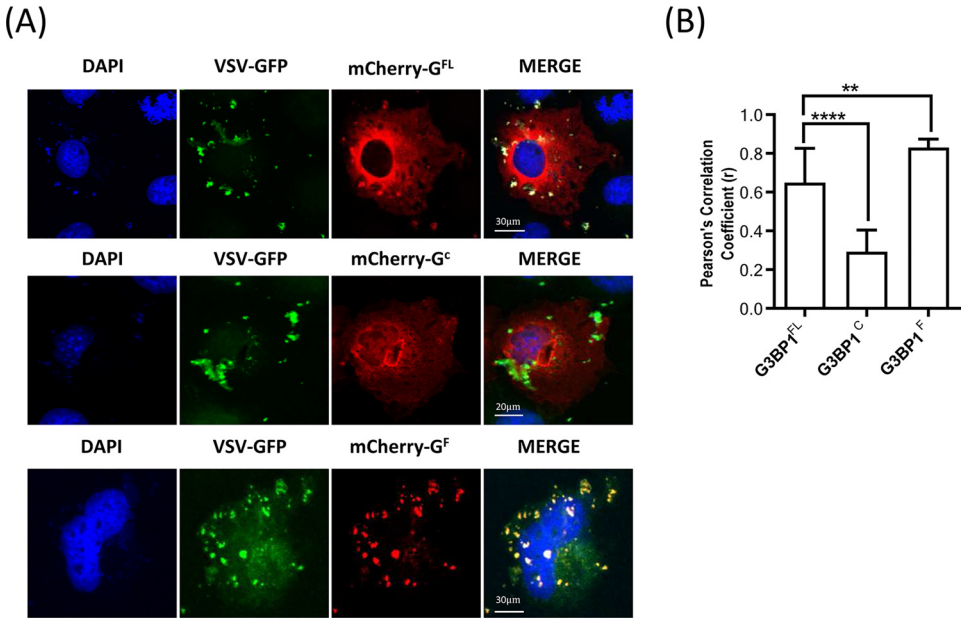

Figure 5. The C-terminal RGG domain of G3BP1 co-localizes with infecting VSV. Confocal microscopy examining the co-localization of mCherry-tagged G3BP1^{FL} (*top panel*), G3BP1^{C} (*middle panel*), or G3BP1^{F} (*bottom panel*) mutants and GFP-tagged VSV. Cos-7 cells were transiently transfected with mCherry-tagged G3BP1^{FL}, G3BP1^{C}, or G3BP1^{F} constructs and 24 h later infected with VSV at a multiplicity of infection of 10. Images were taken 2 h postinfection with VSV. DAPI staining was included to reveal cell nucleus. *B*, Pearson's correlation coefficient (*r*) was used to quantify the degree of co-localization of G3BP1 or its variants with VSV ($n = 10$; current images are reused in Fig. S3 to indicate outline of the cell used to calculate Pearson's correlation coefficient). Statistical significance was analyzed as in Fig. 1. **, $p < 0.005$; ****, $p < 0.0001$).

G3BP1 and G^{F} variant could directly bind poly(I·C) and HCV-dsRNA (Fig. 4*C*). Taken together, our data suggested that the RGG domain of G3BP1 could mediate the direct binding of HCV-dsRNA and poly(I·C), in addition to its binding of RIG-I (Fig. 3*C*).

G3BP1 and its RGG domain associates with infecting vesicular stomatitis virus

We also attempted to visualize the effect of G3BP1 and its RGG domain interactions with infecting viruses. Vesicular stomatitis virus (VSV) is known to induce the formation of SG-like structures in infected cells but unlike rabies virus, it is not known whether G3BP1 is involved (24, 25). VSV is also known to infect mammalian cell lines such as Cos-7 (26). Therefore we transfected Cos-7 cells with mCherry-tagged full-length G3BP1 (G^{FL}) or truncated G^{c} or G^{F} variants, followed by infection of the cells with live GFP-tagged VSV. As shown in Fig. 5*A*, full-length G3BP1 was found to localize in the cytosol and in granule-like structures. GFP-tagged VSV were found to co-localize with a portion of the overexpressed full-length G3BP1 in the granule-like structures in the infected Cos-7 cells (*top panel*). On the other hand, the G^{c} variant was found to be expressed diffusely in the cytosol, and there was significant reduction in the co-localization of VSV with the overexpressed G^{c} variant that lack both the RRM and RGG domains (*central panel*). Interestingly, the overexpressed G^{F} variant was found predominantly to be in granule-like structures (*bottom panel*), and more significantly, most of the G^{F} variant co-localized with the infecting VSV (Fig. 5*B*). These observations suggested that the RGG domain of G3BP1 is responsible for G3BP1 interaction with infecting viruses and also likely, viral content such as their dsRNA.

Computer modeling of RIG-1 and G3BP1 interaction

We showed that G3BP1 could bind RIG-I (Figs. 1*C* and 2*C*) and that this interaction involves G3BP1 RGG domain (Fig. 3*C*). We also demonstrated that the G3BP1 RGG domain co-localizes with infecting VSV (Fig. 5) and could bind viral RNA (Fig. 4, *B* and *C*). It is also known that RIG-I possesses an RNA-binding domain and binds viral RNA (27). To better understand the interactions between G3BP1, RIG-I, and viral dsRNA, we undertook computational modeling of these molecules in complex with each other using available crystal structures of RIG-I and G3BP1. As shown in Fig. 6, the RNA-binding domain of RIG-I was found to juxtapose and bind to the RGG domain of G3BP1. This modeling result correlated well and was also consistent with our data demonstrating that the RGG domain of G3BP1 could bind viral dsRNA and RIG-I. Taken together, the overall data suggested that G3BP1 likely acts as a co-sensor of viral RNA to facilitate and/or enhance RIG-I sensing of these PAMPs.

Discussion

We show in this study that the mammalian stress granule protein G3BP1 plays a critical role in the induction of the RIG-I–mediated type 1 interferon response. We demonstrate that G3BP1 could physically bind RIG-I and synergize with RIG-I to induce the synthesis of *ifn-b* mRNA. Thus, our current data revealed a role for G3BP1 in host anti-viral response by directly participating in RIG-I signaling and inducing IFN-β production. A recent study also suggested that G3BP1 could interact with RIG-I, but in a totally different cellular context, to regulate NFATc activation in arteriosclerotic Wnt signaling (16). Nevertheless, this finding together with ours confirmed that G3BP1

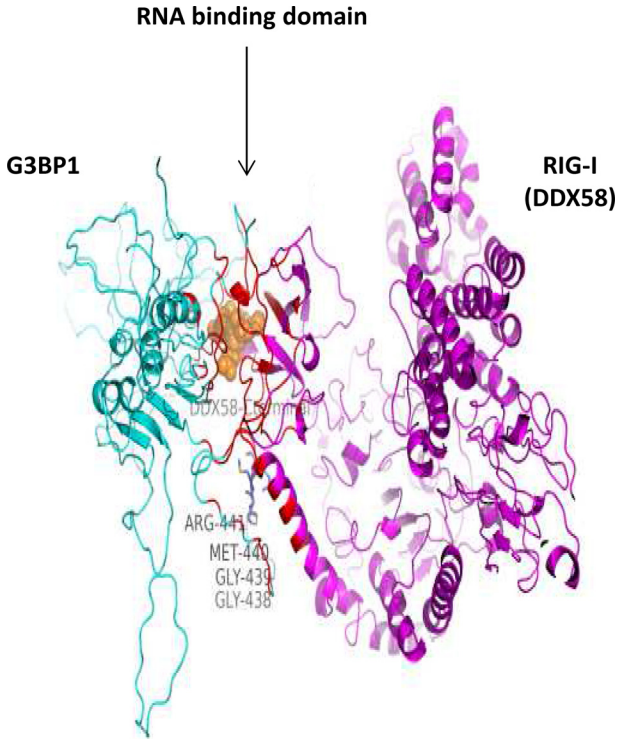

Figure 6. Computational modeling of G3BP1 and RIG-I interaction. Computational modeling of the docking G3BP1 and RIG-I (DDX58) complex. G3BP1 and RIG-I are colored in *cyan* and *purple*, respectively, and with the interacting residues of G3BP1 colored in *red*. The C-terminal of RIG-I is represented in *orange spheres*.

could interact with RIG-I. In addition, our study went one step further by defining the domain within G3BP1 that is necessary for it to bind RIG-I.

G3BP1 is a critical component of the mammalian stress granules and functions by sequestering host mRNA and stalling their translation in times of cell stress (28). We now show that G3BP1 could also bind viral dsRNA from HCV (Fig. 4). Interestingly, G3BP1 binding of host endogenous mRNA involves its RRM domain (19), whereas our finding here indicated that G3BP1 binding of viral dsRNA occurs via its RGG domain. Perhaps this differential binding of host *versus* viral RNA via different domains allows G3BP1 to segregate its function in classical stress granules and anti-viral stress granules. G3BP1 has been shown to possess intrinsic endonuclease/RNase activity against host mRNAs such as in the degradation of c-*myc* mRNA (18), and it remains to be determined whether G3BP1 could exhibit similar enzymatic activity against viral dsRNA. Because RIG-I is known to sense shorter fragments of viral dsRNA (29), it is tempting to speculate that G3BP1 could also function to trim viral dsRNA into shorter lengths to facilitate RIG-I sensing.

Our biochemical data indicated that G3BP1 RGG domain binds viral dsRNA and RIG-I (Figs. 3 and 4). Our computational modeling study suggested that the RNA-binding domain of RIG-I binds G3BP1 (Fig. 6). Hence, a three dimensional model emerges whereby viral dsRNA is bound by and sandwiched between G3BP1 RGG and RIG-I RNA-binding domains. This working model suggested that G3BP1 could serve as a co-sensor of viral dsRNA and facilitates or promotes RIG-I sensing of these PAMPs by directly binding RIG-1 and bringing these PAMPs into proximity for RIG-I signaling. This hypothesis is further strengthen by our time-lapsed confocal microscopy observation showing a spatial redistribution of G3BP1 away from granular structures to the cytosol where RIG-I are in abundance upon tp(I·C) stimulation (Fig. 2, Fig. S2, and Movie S1).

Although our current study focuses on the role of G3BP1 in RIG-I signaling, we did detect weak binding of G3BP1 to DDX41 and c-GAS (Fig. 1*C*). While this manuscript was in revision, a report surfaced to indicate that G3BP1 could also act to promote c-GAS induction of *ifn-b* production (30). The authors also proposed that G3BP1 functioned independently of mammalian SG to promote DNA binding and activation of c-GAS. This finding is consistent with our current study, whereby we showed that G3BP1 binds dsRNA and further enhanced RIG-I induction of *ifn-b* mRNA synthesis. However, unlike our study, these authors were not able to identify any domain within G3BP1 that mediated the interaction with DNA or c-GAS and suggested that only intact G3BP1 could function to promote c-GAS activation. By contrast, we were able to identify the RGG domain of G3BP1 to be necessary for binding dsRNA and RIG-1. Furthermore, our computational study reveals a mechanistic model whereby G3BP1 functions as a co-sensor of RIG-1 in the recognition and binding of viral RNA.

In conclusion, our study has elucidated a role for G3BP1 in promoting and enhancing RIG-I–mediated IFN-β response. Our biochemical and modeling studies further suggested that G3BP1 likely acts as a co-sensor to facilitate RIG-I recognition of pathogenic RNA.

Experimental procedures

Cells, viruses, and reagents

HEK293T, Cos-7, and RAW264.7 cells were cultured in Dulbecco's modified Eagle's medium supplemented with 10% fetal bovine serum, 1% penicillin/streptomycin in 5% CO_2 incubator. Poly(I·C) (Invivogen) was mixed with Lipofectamine 3000 (Thermo Fisher Scientific) and used to transfect cells. Anti-FLAG (M2) beads and anti-FLAG (M2)/anti-HA antibodies were purchased from Sigma. VSV was provided by Y. Zhang (National University of Singapore). Anti-actin antibody (A300-485A) was purchased from Bethyl Laboratories, and anti-RIG-I (SC98911) and anti-G3BP1 (SC70283) antibodies were purchased from Santa Cruz.

Reporter assay

HEK293T cells seeded at a density of 0.5×10^6 cells/well in 12-well plates were transfected with empty vector or expression vectors bearing G3BP1, RIG-I, MAVS, DDX41, c-GAS, or STING along with the reporter vector (100 ng/well) and internal control vector pRL-TK (50 ng/well) (Promega) using Lipofectamine 3000. The *ifn-b* promoter luciferase reporter plasmid was provided by Dr. D. Wang (Zhejiang University, Zhejiang, China). After 48 h of transfection *Firefly* and *Renilla* luciferase activities were measured as described (31) using a dual-luciferase reporter assay kit (Promega).

IP and immunoblot (IB) analyses

HEK293T cells were seeded on 60-mm culture plates (Cornings) at a density of 2.5×10^6 cells/plate. One day later, the cells were transiently transfected with empty vector or various expression vectors using Lipofectamine 3000 kit (Thermo Fisher Scientific). Immunoprecipitation and immunoblot analyses were performed according to the methods as previously described (31).

Cell-free translation system

TNT Quick Coupled transcription/translation system kit (Promega) was used according to the manufacturers' instructions to express $G3BP1^{FL}$, $G3BP1^{F}$, and DDX41. Briefly, the total volume for one reaction was set at 50 μl, and each reaction contained 1 μg of template plasmid. The reaction mixtures were incubated at 30 °C for 90 min, followed by FLAG tag–mediated purification of the *in vitro* translated proteins.

Substrate pulldown assay

The biotin-poly(I·C) and biotin-HCV dsRNA pulldown assays were performed as described (32). In brief, whole cell lysate (WCL) from cells that were transfected with FLAG-tagged RIG-I or DDX41 or G3BP1 was incubated with 1 μg of biotin-conjugated RNA sequence from hepatitis C virus as described (33) (IDT) or commercially available biotin-conjugated poly(I·C) (Invivogen). Subsequently, streptavidin-conjugated magnetic beads (50% w/v) were added to the mixture and incubated on the rotator for 2 h at 4 °C. The beads were washed with cold buffer three times before being resuspended in SDS sample buffer. The substrate pulldown assays were also repeated using *in vitro* translated $G3BP1^{FL}$, $G3BP1^{F}$, and DDX41 proteins.

Confocal microscopy

Cos-7 cells were fixed with 4% paraformaldehyde for 20 min, washed with PBS, permeabilized in 0.5% Triton for 10 min, and washed again with PBS. The cells were blocked with 5% BSA for 1 h and incubated overnight with primary antibodies at 4 °C. After PBS wash, the cells were incubated further with chicken anti-rabbit IgG Alexa Fluor 488, donkey anti-goat IgG Alexa Fluor 633, and streptavidin Alexa Fluor 568 conjugate from Thermo Fisher Scientific. After repeated washing with PBS, cells were finally mounted with ProLong Gold antifade reagent with DAPI (Thermo Fisher Scientific) and scanned using an Olympus confocal laser microscope under 40× or 100× objective.

Computational modeling

Homology models of G3BP1 and RIG-I (DDX58) proteins were predicted using MODELLER 9.16 and protein sequences (Uniprot: P97855) and (Uniprot: Q6Q899). The structures with the lowest PDF scores were picked for docking purposes. The homology models were used to obtain the protein–protein docking complex via ZDOCK online server (http://zdock.umassmed.edu) with the default parameters (34).[4] The first ranking pose was selected for representation and the figure was created using PyMOL software.

[4] Please note that the JBC is not responsible for the long-term archiving and maintenance of this site or any other third party hosted site.

Author contributions—S. S.-Y. K. and K.-P. L. conceptualization; S. S.-Y. K. and L. S. data curation; S. S.-Y. K. and K.-P. L. formal analysis; S. S.-Y. K. and K.-P. L. supervision; S. S.-Y. K., L. S., and K.-P. L. validation; S. S.-Y. K. and K.-P. L. writing-original draft; S. S.-Y. K. and K.-P. L. writing-review and editing; K.-P. L. resources.

Acknowledgments—We thank the members of the laboratory for insightful discussion.

References

1. Yoneyama, M., Kikuchi M., Natsukawa, T., Shinobu, N., Imaizumi, T., Miyagishi, M., Taira, K., Akira, S., and Fujita, T. (2004) The RNA helicase RIG-I has an essential function in double-stranded RNA-induced innate antiviral responses. *Nat. Immunol.* **5,** 730–737 CrossRef Medline
2. Brierley, M. M., and Fish, E. N. (2002) IFN-α/β receptor interactions to biologic outcomes: understanding the circuitry. *J. Interferon Cytokine Res.* **22,** 835–845 CrossRef Medline
3. Schoggins, J. W., and Rice, C. M. (2011) Interferon-stimulated genes and their antiviral effector functions. *Curr. Opin. Virol.* **1,** 519–525 CrossRef Medline
4. Kawai, T., Takahashi, K., Sato, S., Coban, C., Kumar, H., Kato, H., Ishii, K. J., Takeuchi, O., and Akira, S. (2005) IPS-1, an adaptor triggering RIG-I- and Mda5-mediated type I interferon induction. *Nat. Immunol.* **6,** 981–988 CrossRef Medline
5. Lin, R., Heylbroeck, C., Pitha, P. M., and Hiscott, J. (1998) Virus-dependent phosphorylation of the IRF-3 transcription factor regulates nuclear translocation, transactivation potential, and proteasome-mediated degradation. *Mol. Cell. Biol.* **18,** 2986–2996 CrossRef Medline
6. van der Lee, R., Feng, Q., Langereis, M. A., Ter Horst, R., Szklarczyk, R., Netea, M. G., Andeweg, A. C., van Kuppeveld, F. J, and Huynen, M. A. (2015) Integrative genomics-based discovery of novel regulators of the innate antiviral response. *PLoS Comput. Biol.* **11,** e1004553 CrossRef Medline
7. Parker, F., Maurier, F., Delumeau, I., Duchesne, M., Faucher, D., Debussche, L., Dugue, A., Schweighoffer, F., and Tocque, B. (1996) A Ras-GTPase-activating protein SH3-domain-binding protein. *Mol. Cell. Biol.* **16,** 2561–2569 CrossRef Medline
8. Irvine, K., Stirling, R., Hume, D., and Kennedy, D. (2004) Rasputin, more promiscuous than ever: a review of G3BP. *Int. J. Dev. Biol.* **48,** 1065–1077 CrossRef Medline
9. Anderson, P., and Kedersha, N. (2006) RNA granules. *J. Cell Biol.* **172,** 803–808 CrossRef Medline
10. Nover, L., Scharf, K. D, and Neumann, D. (1983) Formation of cytoplasmic heat shock granules in tomato cell cultures and leaves. *Mol. Cell. Biol.* **3,** 1648–1655 CrossRef Medline
11. Onomoto, K., Jogi, M., Yoo, J. S., Narita, R., Morimoto, S., Takemura, A., Sambhara, S., Kawaguchi, A., Osari, S., Nagata, K., Matsumiya, T., Namiki, H., Yoneyama, M., and Fujita, T. (2012) Critical role of an antiviral stress granule containing RIG-I and PKR in viral detection and innate immunity. *PLoS One* **7,** e43031 CrossRef Medline
12. Cobos Jiménez, V, Martinez, F. O., Booiman, T., van Dort, K. A., van de Klundert, M. A., Gordon, S., Geijtenbeek, T. B, and Kootstra, N., A. (2015) G3BP1 restricts HIV-1 replication in macrophages and T-cells by sequestering viral RNA. *Virology* **486,** 94–104 CrossRef Medline
13. Dougherty, J. D, Tsai, W. C., and Lloyd, R. E. (2015) Multiple poliovirus proteins repress cytoplasmic RNA granules. *Viruses* **7,** 6127–6140 CrossRef Medline
14. Ng, C. S., Jogi, M., Yoo, J. S., Onomoto, K., Koike, S., Iwasaki, T., Yoneyama, M., Kato, H., and Fujita, T. (2013) Encephalomyocarditis virus disrupts stress granules, the critical platform for triggering antiviral innate immune responses. *J. Virol.* **87,** 9511–9522 CrossRef Medline
15. Loo, Y. M., Fornek, J., Crochet, N., Bajwa, G., Perwitasari, O., Martinez-Sobrido, L., Akira, S., Gill, M. A., García-Sastre, A., Katze, M. G., and Gale,

M., Jr. (2008) Distinct RIG-I and MDA5 signaling by RNA viruses in innate immunity. *J. Virol.* **82,** 335–345 CrossRef Medline
16. Ramachandran, B., Stabley, J. N., Cheng, S. L., Behrmann, A. S., Gay, A., Li, L., Mead, M., Kozlitina, J., Lemoff, A., Mirzaei, H., Chen, Z., and Towler, D. A. (2018) A GTPase-activating protein-binding protein (G3BP1)/antiviral protein relay conveys arteriosclerotic Wnt signals in aortic smooth muscle cells. *J. Biol. Chem.* **293,** 7942–7968 CrossRef Medline
17. Tourrière, H., Chebli, K., Zekri, L., Courselaud, B., Blanchard, J. M., Bertrand, E., and Tazi, J. (2003) The RasGAP-associated endoribonuclease G3BP assembles stress granules. *J. Cell Biol.* **160,** 823–831 CrossRef Medline
18. Gallouzi, I. E., Parker, F., Chebli, K., Maurier, F., Labourier, E., Barlat, I., Capony, J. P., Tocque, B., and Tazi, J. (1998) A novel phosphorylation-dependent RNase activity of GAP-SH3 binding protein: a potential link between signal transduction and RNA stability. *Mol. Cell. Biol.* **18,** 3956–3965 CrossRef Medline
19. Tourrière, H., Gallouzi, I. E., Chebli, K., Capony, J. P., Mouaikel, J., van der Geer, P., and Tazi, J. (2001) RasGAP-associated endoribonuclease G3Bp: selective RNA degradation and phosphorylation-dependent localization. *Mol. Cell. Biol.* **21,** 7747–7760 CrossRef Medline
20. Kedersha, N., Panas, M. D., Achorn, C. A., Lyons, S., Tisdale, S., Hickman, T., Thomas, M., Lieberman, J., McInerney, G. M., Ivanov, P., and Anderson, P. (2016) G3BP–Caprin1–USP10 complexes mediate stress granule condensation and associate with 40S subunits. *J. Cell Biol.* **212,** 845–860 CrossRef Medline
21. Ozdilek, B. A., Thompson, V. F., Ahmed, N. S., White, C. I., Batey, R. T., and Schwartz, J. C. (2017) Intrinsically disordered RGG/RG domains mediate degenerate specificity in RNA binding. *Nucleic Acids Res.* **45,** 7984–7996 CrossRef Medline
22. Yagi, R., Miyazaki, T., and Oyoshi, T. (2018) G-quadruplex binding ability of TLS/FUS depends on the β-spiral structure of the RGG domain. *Nucleic Acids Res.* **46,** 5894–5901 CrossRef Medline
23. Solomon, S., Xu, Y., Wang, B., David, M. D., Schubert, P., Kennedy, D., and Schrader, J. W. (2007) Distinct structural features of caprin-1 mediate its interaction with G3BP-1 and its induction of phosphorylation of eukaryotic translation initiation factor 2α, entry to cytoplasmic stress granules, and selective interaction with a subset of mRNAs. *Mol. Cell. Biol.* **27,** 2324–2342 CrossRef Medline
24. Dinh, P. X., Beura, L. K., Das, P. B., Panda, D., Das, A., and Pattnaik, A. K. (2013) Induction of stress granule-like structures in vesicular stomatitis virus-infected cells. *J. Virol.* **87,** 372–383 CrossRef Medline
25. Nikolic, J., Civas, A., Lama, Z., Lagaudrière-Gesbert, C, and Blondel, D. (2016) Rabies virus infection induces the formation of stress granules closely connected to the viral factories. *PLoS Pathog.* **12,** e1005942 CrossRef Medline
26. Gadaleta, P., Vacotto, M., and Coulombié, F. (2002) Vesicular stomatitis virus induces apoptosis at early stages in the viral cycle and does not depend on virus replication. *Virus Res.* **86,** 87–92 CrossRef Medline
27. Lu, C., Ranjith-Kumar, C. T., Hao, L., Kao, C. C., and Li, P. (2011) Crystal structure of RIG-I C-terminal domain bound to blunt-ended double-strand RNA without 5′ triphosphate. *Nucleic Acids Res.* **39,** 1565–1575 CrossRef Medline
28. Protter, D. S. W., and Parker, R. (2016) Principles and properties of stress granules. *Trends Cell Biol.* **26,** 668–679 CrossRef Medline
29. Kato, H., Takeuchi, O., Mikamo-Satoh, E., Hirai, R., Kawai, T., Matsushita, K., Hiiragi, A., Dermody, T. S., Fujita, T., and Akira, S. (2008) Length-dependent recognition of double-stranded ribonucleic acids by retinoic acid-inducible gene-I and melanoma differentiation-associated gene 5. *J. Exp. Med.* **205,** 1601–1610 CrossRef Medline
30. Liu, Z. S., Cai, H., Xue, W., Wang, M., Xia, T., Li, W. J., Xing, J. Q., Zhao, M., Huang, Y. J., Chen, S., Wu, S. M., Wang, X., Liu, X., Pang, X., Zhang, Z. Y., *et al.* (2019) G3BP1 promotes DNA binding and activation of cGAS. *Nat. Immunol.* **20,** 18–28 CrossRef Medline
31. Kim, S. S., Lee, K. G., Chin, C. S., Ng, S. K., Pereira, N. A., Xu, S., and Lam, K. P. (2014) DOK3 is required for IFN-β production by enabling TRAF3/TBK1 complex formation and IRF3 activation. *J. Immunol.* **193,** 840–848 CrossRef Medline
32. Lee, K. G., Kim, S. S., Kui, L., Voon, D. C., Mauduit, M., Bist, P., Bi, X., Pereira, N. A., Liu, C., Sukumaran, B., Rénia, L., Ito, Y., and Lam, K. P. (2015) Bruton's tyrosine kinase phosphorylates DDX41 and activates its binding of dsDNA and STING to initiate type 1 interferon response. *Cell Rep.* **10,** 1055–1065 CrossRef Medline
33. Oshiumi, H., Ikeda, M., Matsumoto, M., Watanabe, A., Takeuchi, O., Akira, S., Kato, N., Shimotohno, K., and Seya, T. (2010) Hepatitis C virus core protein abrogates the DDX3 function that enhances IPS-1–mediated IFN-β induction. *PLoS One* **5,** e14258 CrossRef Medline
34. Pierce, B. G., Wiehe, K., Hwang, H., Kim, B. H., Vreven, T., and Weng, Z. (2014) ZDOCK Server: interactive docking prediction of protein–protein complexes and symmetric multimers. *Bioinformatics* **30,** 1771–1773 CrossRef Medline

The stress granule protein G3BP1 binds viral dsRNA and RIG-I to enhance interferon- β response

Susana Soo-Yeon Kim, Lynette Sze and Kong-Peng Lam

J. Biol. Chem. 2019, 294:6430-6438.
doi: 10.1074/jbc.RA118.005868 originally published online February 25, 2019

VOLUME 294 (2019) PAGES 6430–6438
DOI 10.1074/jbc.AAC119.009397

Correction: The stress granule protein G3BP1 binds viral dsRNA and RIG-I to enhance interferon-β response.

Susana Soo-Yeon Kim, Lynette Sze, ChengCheng Liu, and Kong-Peng Lam

ChengCheng Liu was inadvertently omitted from the author list. The corrected list is shown above.